Comparisons of the NGA Ground-Motion Relations

Norman Abrahamson,[a)] M.EERI, Gail Atkinson,[b)] M.EERI, David Boore,[c)] Yousef Bozorgnia,[d)] M.EERI, Kenneth Campbell,[e)] M.EERI, Brian Chiou,[f)] I. M. Idriss,[g)] M.EERI, Walter Silva,[h)] M.EERI, and Robert Youngs,[i)] M.EERI

The data sets, model parameterizations, and results from the five NGA models for shallow crustal earthquakes in active tectonic regions are compared. A key difference in the data sets is the inclusion or exclusion of aftershocks. A comparison of the median spectral values for strike-slip earthquakes shows that they are within a factor of 1.5 for magnitudes between 6.0 and 7.0 for distances less than 100 km. The differences increase to a factor of 2 for M5 and M8 earthquakes, for buried ruptures, and for distances greater than 100 km. For soil sites, the differences in the modeling of soil/sediment depth effects increase the range in the median long-period spectral values for M7 strike-slip earthquakes to a factor of 3. The five models have similar standard deviations for M6.5-M7.5 earthquakes for rock sites and for soil sites at distances greater than 50 km. Differences in the standard deviations of up to 0.2 natural log units for moderate magnitudes at all distances and for large magnitudes at short distances result from the treatment of the magnitude dependence and the effects of nonlinear site response on the standard deviation. [DOI: 10.1193/1.2924363]

INTRODUCTION

As part of the NGA project, five groups developed new ground-motion models for application to the shallow crustal earthquakes in the Western United States (WUS). The models are described in five accompanying papers: Abrahamson and Silva, 2008 (AS08); Boore and Atkinson, 2008 (BA08); Campbell and Bozorgnia, 2008 (CB08); Chiou and Youngs, 2008 (CY08); and Idriss, 2008 (I08). In this paper, we compare the data sets, model parameterizations, use of analytical model constrains, and the resulting ground motions (median and aleatory variability) from the five NGA models. The ob-

[a)] Pacific Gas & Electric Company, 245 Market Street, San Francisco, CA 94105
[b)] Department of Earth Sciences, University of Western Ontario, London, Ont. Canada N6A 5B7
[c)] U.S. Geological Survey, MS977, 345 Middlefield Rd., Menlo Park, CA 94025
[d)] Pacific earthquake Engineering Center, University of California, Berkeley, CA, 94720
[e)] ABS Consulting/EQECAT, 1130 NW 161st Pl., Beaverton, OR 97006-6337
[f)] Division of Research and Innovation, California Department of Transportation, Sacramento, CA
[g)] Professor Emeritus, University of California, Davis
[h)] Pacific Engineering and Analysis, El Cerrito, CA 94546
[i)] Geomatrix Consultants Inc., 2101 Webster St., 12th Floor, Oakland CA 94612

Earthquake Spectra, Volume 24, No. 1, pages 45–66, February 2008;

Table 1. Summary of data sets used by the developers

	AS08	BA08	CB08	CY08	I08
Number of Earthquakes	135	58	64	125	72
Number of Recordings	2754	1574	1561	1950	942

jective of this paper is to compare the five NGA models and provide some explanations for the causes of the differences, but not to evaluate the strengths and weaknesses of the different models.

DATA SET SELECTION

Although the NGA developers all started with the same data base of 3551 recordings from 173 earthquakes, the selected data sets used to develop the models have significant differences. The number of selected earthquakes and recordings are summarized in Table 1. A key difference in the data sets is the treatment of aftershocks. The AS08 and CY08 data sets include aftershocks, resulting in a much larger number of earthquakes than the BA08 and CB08 sets. The I08 data set includes aftershocks, but is has the smallest number of recordings because it only includes rock sites ($450\ \mathrm{m/s} < V_{S30} < 900\ \mathrm{m/s}$). The earthquakes selected by each developer team and the number of recordings for each earthquake is listed in Table 2.

An important issue in the selection of the earthquakes was the applicability of the well-recorded large-magnitude earthquakes from outside of the WUS (1999 Chi-Chi and 1999 Kocaeli) to the prediction of ground motions in the WUS. All of the developers considered both the Chi-Chi and Kocaeli data to be applicable to the WUS. Furthermore, comparisons of the NGA models with Eurpoean data have shown that the NGA models are applicable to Europe (Campbell and Bozorgnia 2006 and Stafford et al. 2007), suggesting that the NGA models are globally applicable to shallow crustal earthquakes in active tectonic regions.

MODEL FUNCTIONAL FORMS

The main features of the functional forms of the five NGA models are summarized in Table 3. Saturation at short distances is a feature of ground motion models that leads to weaker magnitude scaling at short distances than compared to the magnitude scaling at larger distances. Saturation causes a pinching of the ground motion for different magnitudes at short distance. This is not the same as including a quadratic magnitude scaling that applies at all distances. In ground motion studies, a model is said to have "full saturation" if there is no magnitude scaling of the median ground motion at zero distance. A model is said to have over-saturation if the median ground motion decreases with increasing magnitude at zero distance. All of the NGA models include some form of saturation of the short-period ground motion at short distances through either a magnitude-dependent distance slope (AS08, BA08, CB08, I08) or a magnitude-dependent fictitious

Table 2. Selected earthquakes and number of stations used by the developers

EQID	YEAR	Earthquake Name	Mag	AS08	BA08	CB08	CY08	I08
12	1952	Kern County	7.36	1		1		
20	1957	San Francisco	5.28	1			1	1
25	1966	Parkfield	6.19	4	4	4	4	1
28	1968	Borrego Mtn	6.63	1	2			
29	1970	Lytle Creek	5.33	10		10	7	5
30	1971	San Fernando	6.61	35	31	33	22	10
31	1972	Managua, Nicaragua-01	6.24	1		1	1	
32	1972	Managua, Nicaragua-02	5.20	1			1	
33	1973	Point Mugu	5.65	1			1	
34	1974	Hollister-03	5.14	2	2		2	
35	1975	Northern Calif-07	5.20	5				
36	1975	Oroville-01	5.89	1			1	1
37	1975	Oroville-02	4.79	2			2	
38	1975	Oroville-04	4.37	3			3	
39	1975	Oroville-03	4.70	9			9	2
40	1976	Friuli, Italy-01	6.50	4	5	5	3	1
41	1976	Gazli, USSR	6.80	1		1	1	1
42	1976	Fruili, Italy-03	5.50	3			3	1
43	1976	Friuli, Italy-02	5.91	4			4	1
44	1977	Izmir, Turkey	5.30				1	
45	1978	Santa Barbara	5.92	1			1	
46	1978	Tabas, Iran	7.35	4	7	7	3	2
47	1979	Dursunbey, Turkey	5.34	1			1	1
48	1979	Coyote Lake	5.74	10	7	10	10	1
49	1979	Norcia, Italy	5.90	2	3	3	3	1
50	1979	Imperial Valley-06	6.53	33	33	33	33	1
51	1979	Imperial Valley-07	5.01	16			16	
52	1979	Imperial Valley-08	5.62	1			1	
53	1980	Livermore-01	5.80	6	5	5	6	1
54	1980	Livermore-02	5.42	7			7	2
55	1980	Anza (Horse Canyon)-01	5.19	5	5	5	5	2
56	1980	Mammoth Lakes-01	6.06	3	2	3	3	
57	1980	Mammoth Lakes-02	5.69	3			3	
58	1980	Mammoth Lakes-03	5.91	4			4	
59	1980	Mammoth Lakes-04	5.70	3			4	
60	1980	Mammoth Lakes-05	5.70	2			2	
61	1980	Mammoth Lakes-06	5.94	5			5	
62	1980	Mammoth Lakes-07	4.73	6			6	
63	1980	Mammoth Lakes-08	4.80	7			7	
64	1980	Victoria, Mexico	6.33	4	4	4	4	1
65	1980	Mammoth Lakes-09	4.85	9			9	
68	1980	Irpinia, Italy-01	6.90	12	12	12	12	5
69	1980	Irpinia, Italy-02	6.20	10			10	4

Table 2. (cont.)

EQID	YEAR	Earthquake Name	Mag	AS08	BA08	CB08	CY08	I08
70	1981	Irpinia, Italy-03	4.70	1			1	
71	1981	Taiwan SMART1(5)	5.90	7				
72	1981	Corinth, Greece	6.60	1		1	1	
73	1981	Westmorland	5.90	6	6	6	6	
74	1983	Mammoth Lakes-10	5.34	1			1	
75	1983	Mammoth Lakes-11	5.31	1			1	
76	1983	Coalinga-01	6.36	45	44	45	45	1
77	1983	Coalinga-02	5.09	20			20	1
78	1983	Coalinga-03	5.38	3			3	1
79	1983	Coalinga-04	5.18	11			11	1
80	1983	Coalinga-05	5.77	9			11	1
81	1983	Coalinga-06	4.89	2			2	1
82	1983	Coalinga-07	5.21	2			2	1
83	1983	Ierissos, Greece	6.70	1			1	
84	1983	Trinidad offshore	5.70	2				
85	1983	Coalinga-08	5.23	2			2	1
86	1983	Taiwan SMART1(25)	6.50	9				
87	1983	Borah Peak, ID-01	6.88	2	2	2		
88	1983	Borah Peak, ID-02	5.10	3			3	2
89	1984	New Zealand-01	5.50				1	
90	1984	Morgan Hill	6.19	27	24	27	26	5
91	1984	Lazio-Abruzzo, Italy	5.80	5	5	5	5	1
94	1984	Bishop (Rnd Val)	5.82	1			1	
95	1985	Taiwan SMART1(33)	5.80	7				
96	1985	Drama, Greece	5.20	1			1	
97	1985	Nahanni, Canada	6.76	3		3	3	3
98	1986	Hollister-04	5.45	3	3	3	3	1
99	1986	Mt. Lewis	5.60	1			1	
100	1986	Taiwan SMART1(40)	6.32	8				
101	1986	N. Palm Springs	6.06	32	30	31	30	6
102	1986	Chalfant Valley-01	5.77	5	5	5	5	
103	1986	Chalfant Valley-02	6.19	11	10	11	11	
104	1986	Chalfant Valley-03	5.65	3			3	
105	1986	Chalfant Valley-04	5.44	2			2	
108	1986	San Salvador	5.80	2	2		2	1
110	1987	Baja California	5.50				1	1
111	1987	New Zealand-02	6.60	2		2	2	
112	1987	New Zealand-03	5.80				1	
113	1987	Whittier Narrows-01	5.99	108	106	109	105	10
114	1987	Whittier Narrows-02	5.27	9		10	11	2
115	1987	Superstition Hills-01	6.22	1		1	1	
116	1987	Superstition Hills-02	6.54	11	11	11	11	
117	1988	Spitak, Armenia	6.77	1			1	

Table 2. (cont.)

EQID	YEAR	Earthquake Name	Mag	AS08	BA08	CB08	CY08	I08
118	1989	Loma Prieta	6.93	77	73	77	58	22
119	1990	Griva, Greece	6.10	1		1	1	
120	1991	Georgia, USSR	6.20	5			5	
121	1992	Erzican, Turkey	6.69	1		1	1	
122	1992	Roermond, Netherlands	5.30	2	3		1	3
123	1992	Cape Mendocino	7.01	6	6	6	6	
124	1992	New Zealand-04	5.70				1	
125	1992	Landers	7.28	68	68	67	16	3
126	1992	Big Bear-01	6.46	38	39	38	18	5
127	1994	Northridge-01	6.69	155	154	149	134	28
128	1994	Double Springs	5.90	1			1	
129	1995	Kobe, Japan	6.90	20	12	22	17	5
130	1995	Kozani, Greece-01	6.40	3	3	3	1	2
131	1995	Kozani, Greece-02	5.10	2			1	
132	1995	Kozani, Greece-03	5.30	2			1	
133	1995	Kozani, Greece-04	5.10	2			1	
134	1995	Dinar, Turkey	6.40	2	4	2	2	
136	1999	Kocaeli, Turkey	7.51	17	26	22	17	6
137	1999	Chi-Chi, Taiwan	7.62	318	380	381	208	152
138	1999	Duzce, Turkey	7.14	13	22	14	12	7
139	1972	Stone Canyon	4.81	3			3	1
140	1972	Sitka, Alaska	7.68	1		1	1	1
141	1976	Caldiran, Turkey	7.21	1		1	1	
142	1979	St. Elias, Alaska	7.54		2	2		
143	1990	Upland	5.63	3	3	3	2	1
144	1990	Manjil, Iran	7.37	5	7	7	3	1
145	1991	Sierra Madre	5.61	9	8	8	9	1
147	1994	Northridge-02	6.05	15			18	4
148	1994	Northridge-03	5.20	7			7	3
149	1994	Northridge-04	5.93	7			7	1
150	1994	Northridge-05	5.13	8			8	3
151	1994	Northridge-06	5.28	48			46	12
152	1992	Little Skull Mtn,NV	5.65	8	8	8	5	3
153	1997	Northwest China-01	5.90	2	2			
154	1997	Northwest China-02	5.93	2	2			
155	1997	Northwest China-03	6.10	1				
156	1997	Northwest China-04	5.80	2	2			
157	1998	San Juan Bautista	5.17	1			1	
158	1999	Hector Mine	7.13	79	82	78	15	12
160	2000	Yountville	5.00	24	24	24	18	3
161	2001	Big Bear	4.53	42	41	43	39	2
162	2001	Mohawk Val, Portola	5.17	6	6	6	3	
163	2001	Anza-02	4.92	72	72	72	34	11

Table 2. (cont.)

EQID	YEAR	Earthquake Name	Mag	AS08	BA08	CB08	CY08	I08
164	2001	Gulf of California	5.70	11	11	11		
165	2002	CA/Baja Border Area	5.31	9	9	9	6	
166	2002	Gilroy	4.90	34	34	34	18	10
167	2002	Yorba Linda	4.27	12	12	12	12	
		Nenana Mountain,						1
168	2002	Alaska	6.70	5	33	5		
169	2002	Denali, Alaska	7.90	9	23	9	4	
170	2003	Big Bear City	4.92	35	33	36	25	6
171	1999	Chi-Chi, Taiwan-02	5.90	195			127	122
172	1999	Chi-Chi, Taiwan-03	6.20	189			120	104
173	1999	Chi-Chi, Taiwan-04	6.20	202			123	93
174	1999	Chi-Chi, Taiwan-05	6.20	166			100	117
175	1999	Chi-Chi, Taiwan-06	6.30	188			135	112

depth (CY08). In several cases, the selected data sets would have lead to over-saturation of the short-period ground motion at short distances if the regression was unconstrained, but none of the developers allowed over-saturation in their models.

The five models all include a style-of-faulting factor, but the grouping of the normal/oblique slip events with either normal or strike-slip events is different (Table 4). Three models (AS08, CB08, and CY08) include rupture-depth and hanging-wall (HW) factors. The BA08 model implicitly includes these effects through the use of R_{JB} as the primary distance measure. The I08 model does not include either of these effects.

There is a correlation between the style-of-faulting effect and the rupture-depth effect because, in the NGA data base, a greater fraction of reverse earthquakes are buried ruptures as compared to strike-slip earthquakes. For the three models that include the rupture-depth parameter, much of the style-of-faulting effect given in previous models is accommodated by the rupture-depth effect.

Four of the five models are applicable to soil sites as well as rock sites; the I08 model is only applicable for rock sites. All four models applicable to soil sites include nonlinear site amplification factors. Three models (AS08, BA08, and CB08) constrained the nonlinear part of the amplification using either analytical model results or other published nonlinear amplification factors. In contrast, the CY08 model derived the nonlinear amplification directly from the NGA data as part of the regression.

The soil/sediment depth information is missing for most of the recording sites in the NGA data set, causing difficulties in developing models for this effect. Three models (AS08, CB08, and CY08) included the soil/sediment depth effects and one model (BA08) did not include soil/sediment depth effects. The AS08 model constrained the shallow soil/sediment depth scaling using analytical results from 1-D site amplification and constrained the deep soil/sediment depth scaling using analytical results from 3-D

Table 3. Functional forms of NGA models

	AS08	BA08	CB08	CY08	I08
Saturation at short distances	X	X	X	X	X
Style-of-faulting factor	X	X	X	X	X
Rupture depth factor	X	Implicit through R_{JB}	X (RV only)	X	
HW factor	X	Implicit through R_{JB}	X	X	
Nonlinear site amplification	Constrained (Walling et al., 2008)	Constrained (Choi & Stewart, 2005)	Constrained (Walling et al., 2008)	X	N/A
Soil/sediment depth factor	Constrained (Shallow: Silva, 2005; deep: Day et al., 2005)		Constrained deep: Day et al. (2005)	X	N/A
Magnitude dependent σ	X			X	X
Nonlinear effects on σ	Intra-event and intra-event terms		Intra-event term only	Intra-event and intra-event terms	

Table 4. Style-of-faulting classification for the NGA models

Style-of-Faulting Class	AS08	BA08	CB08	CY08	I08
Normal	NML	NML & NML/OBL	NML & NML/OBL	NML	
	$-90 \le \text{rake} \le -60$	$-90 \le \text{rake} \le -30$	$-90 \le \text{rake} \le -30$	$-90 \le \text{rake} \le -60$	
Strike-Slip	SS & NML/OBL	SS	SS	SS & NML/OBL	SS, NML/OBL, & NML
	$-60 < \text{rake} < 30$	$-30 < \text{rake} < 30$	$-30 < \text{rake} < 30$	$-60 < \text{rake} < 30$	$-90 < \text{rake} < 30$
Reverse	RV & RV/OBL	RV & RV/OBL	RV & RV/OBL	RV & RV/OBL	RV & RV/OBL
	$30 \le \text{rake} \le 90$	$30 \le \text{rake} \le 90$	$30 \le \text{rake} \le 90$	$30 \le \text{rake} \le 90$	$30 \le \text{rake} \le 90$

Table 5. Parameters used in the NGA models

Parameter	AS08	BA08	CB08	CY08	I
Moment magnitude	M	M	M	M	M
Depth-to-top-of-rupture (km)	Z_{TOR}		Z_{TOR}	Z_{TOR}	
Reverse style-of-faulting flag	F_{RV}	RS	F_{RV}	F_{RV}	F
Normal style-of-faulting flag	F_{NM}	NS	F_{NM}	F_{NM}	
Strike-slip style-of-faulting flag		SS			
Unspecified style-of-faulting flag		US			
Aftershock flag	F_{AS}			AS	
Dip (degrees)	δ[a]		δ[a]	δ[a]	
Down-dip rupture width (km)	W[a]				
Closest distance to the rupture plane (km)	R_{rup}		R_{rup}	R_{rup}	R_{rup}
Horizontal distance to the surface projection of the rupture (km)	R_{jb}[a]	R_{jb}	R_{jb}[a]	R_{jb}[a]	
Horizontal distance to the top edge of the rupture measured perpendicular to strike (km)	R_x[a]			R_x[a]	
Hanging Wall Flag	F_{HW}			F_{HW}	
Average shear-wave velocity in the top 30 m (m/s)	V_{S30}	V_{S30}	V_{S30}	V_{S30}	
Depth to $V_S = 1.0$ km/s (km)	$Z_{1.0}$			$Z_{1.0}$	
Depth to $V_S = 2.5$ km/s (km)			$Z_{2.5}$		
Rock motion PGA for nonlinear site response	$\hat{PGA}_{1100}$	pga4nl	A_{1100}		
Rock motion Sa for nonlinear site response				$y_{ref}(T)$	
V_{S30} of rock motion used for nonlinear site response (m/s)	1100	760	1100	1130	

[a] Used for HW scaling only

basin amplification. The CY08 models estimated the soil/sediment depth scaling from the NGA data with available soil/sediment depths. The CB08 model constrained the soil/sediment depth scaling using the results from the 3-D simulations with additional empirical adjustments at short periods and shallow soil/sediment depths.

There are two main differences in the forms of the standard deviation models: magnitude dependence and nonlinear site response effects. Three of the models (AS08, CY08, and I08) have magnitude-dependent standard deviations and two models (BA08, and CB08) have magnitude-independent standard deviations. Of the four models applicable to soil sites, three models (AS08, CB08, and CY08) include some or all of the effects of nonlinear site amplification effects on the standard deviation. The fourth model, BA08, does not consider the effects of nonlinear amplification on the standard deviation. The I08 model does not address this issue since it is only for rock sites.

MODEL PARAMETERS

The model parameters used by each developer are summarized in Table 5. The I08 model, which is only for rock sites, has the simplest parameterization: magnitude, distance, and style-of-faulting. The BA08 model has the next simplest parameterization; in addition to magnitude, distance, and style-of-faulting, it has the added parameters of V_{S30} and input rock motion to model nonlinear site response. The AS08, CB08, and CY08 models have the most complex parameterizations. These models include additional parameters as part of the models for HW effects, rupture-depth effects, and soil/sediment depth effects.

All five models are based on moment magnitude and all five models include a style-of-faulting factors, but the I08 model does not distinguish between strike-slip and normal earthquakes. For the three models that include rupture-depth effects (AS08, CB08, and CY08), the rupture depth is parameterized by the depth to the top of the rupture. Of the three models that included aftershocks (AS08, CY08, and I08), the AS08 and CY08 models account for differences between the median ground motion for aftershocks and mainshocks, with aftershocks having smaller ground motions than mainshocks.

There are two different primary distance measures used. The BA08 model uses the closest horizontal distance to the surface projection of the rupture plane, R_{JB}. The other four models use the closest distance to the rupture plane, R_{rup}. For the HW effect, the AS08, CB08, and CY08 models use additional distance metrics to smooth the HW factor. All three models use the R_{JB} distance in the HW scaling. The AS08 and CY08 models also use a third distance metric, R_x, as part of the HW scaling. The R_x distance is defined as the horizontal distance from the top edge of the rupture, measured perpendicular to the fault strike (R_x is positive over the hanging wall and negative over the footwall).

All of the models except for I08 use the average shear-wave velocity in the top 30 m, V_{S30}, as the primary site parameter. All four models that include site effects incorporate nonlinear site response. Two different measures for the strength of the shaking are used for the nonlinear site response effects: AS08, BA08, and CB08 use the median peak acceleration on a rock outcrop; CY08 use the median spectral acceleration on a rock out-

crop at the period of interest. The BA08 model defines the input rock motion based on V_{S30}=760 m/s whereas the other three models use a V_{S30} of about 1100 m/s. Three models include the soil depth as an additional site parameter: AS08 and CY08 use the depth to V_S=1.0 km/s and CB08 use the depth the V_S=2.5 km/s.

COMPARISON OF THE MEDIAN VALUES

The NGA models use different source parameters and distance measures. Some of the models include the depth to top of rupture as a source parameter. To compare with the NGA models that do not include this parameter, the median depth-to-top-of-rupture from the NGA data base was used: 6 km for M=5.0, 3 km for M=6, 1 km for M=7, and 0 km for M=8.0. To address the different distance measures used by the NGA models, the ground motions were computed for specified source-site geometries.

There is also an issue of the soil/sediment depth to be used for the comparisons. The AS08 and CY08 models both give recommended values of $Z_{1.0}$ to be used if the soil/sediment depth is not known. The relations for the median $Z_{1.0}$ for a given V_{S30} are not consistent between these two models. For the general comparisons, the recommended median $Z_{1.0}$ values are used for each model. For the CB08 model, which uses $Z_{2.5}$ as the soil/sediment depth parameter, the recommendation is to estimate $Z_{2.5}$ from the $Z_{1.0}$. For the comparisons, the $Z_{2.5}$ are estimated using the AS08 estimates of $Z_{1.0}$.

DISTANCE SCALING

The distance scaling for the median ground motion for vertical strike-slip faults and a rock site condition (V_{S30}=760 m/s, $Z_{1.0}$=0.034 km for AS08, $Z_{1.0}$=0.024 km for CY08, $Z_{2.5}$=0.64 km) is compared in Figures 1a and 1b for peak acceleration and T=1 sec spectral acceleration, respectively. For M6 and M7 earthquakes, the five NGA models lead to similar ground motions (within a range of a factor of 1.5). At M5 and M8, the differences between the NGA models become larger (up to a factor of 2) due to the sparse amount strong motion data from M5 and M8 earthquakes.

The large range of the M5 models is due to the selection of the sparse strong motion data from M5 earthquakes. A large set of M5 data is available from broadband network stations, but the compilation of data from moderate magnitude (M5) earthquakes was not emphasized in the NGA project because these earthquakes are generally not of engineering interest in California. The range of the ground motion models for M5 could be greatly reduced with the compilation of the available M5 ground motion recordings.

The distance scaling for soil sites is shown in Figures 2a and 2b for PGA and T=1 sec spectral acceleration, respectively. The range of the soil-site ground motions for the four NGA models applicable to soil sites are similar to the range of ground motions seen for rock sites.

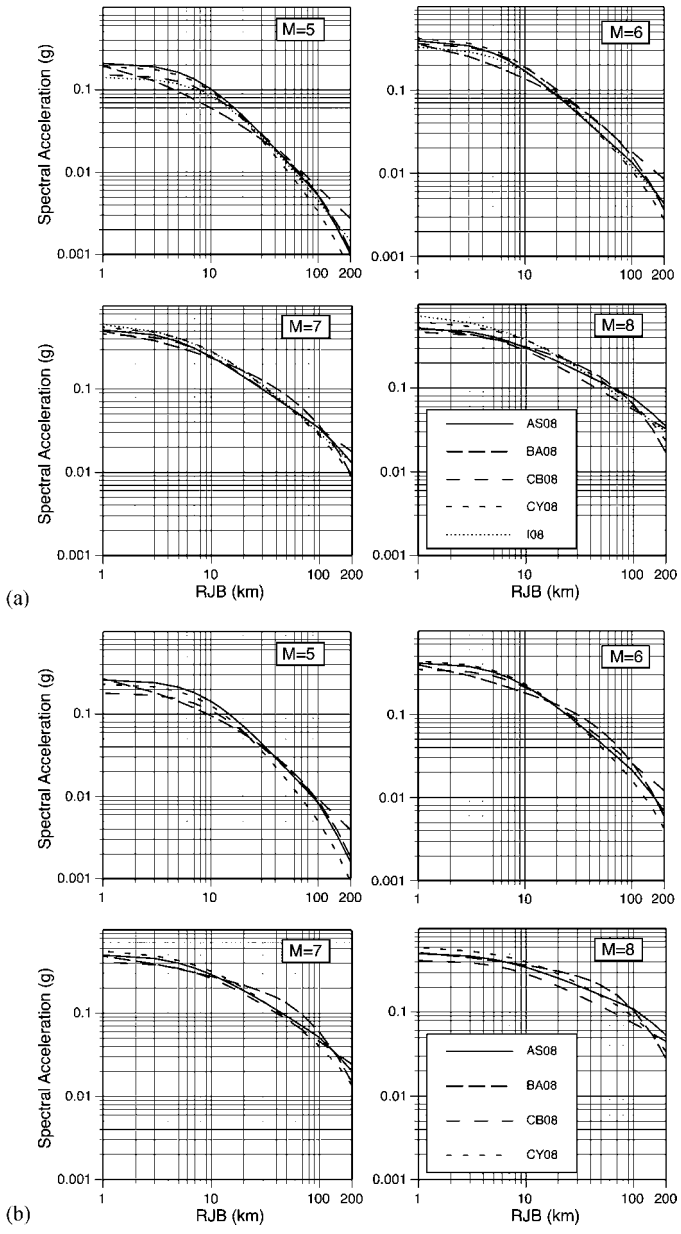

Figure 1. a. Comparison of distance scaling of PGA for strike-slip earthquakes for V_{S30}=760 m/s. b. Comparison of distance scaling of T=1 sec for strike-slip earthquakes for V_{S30}=760 m/s.

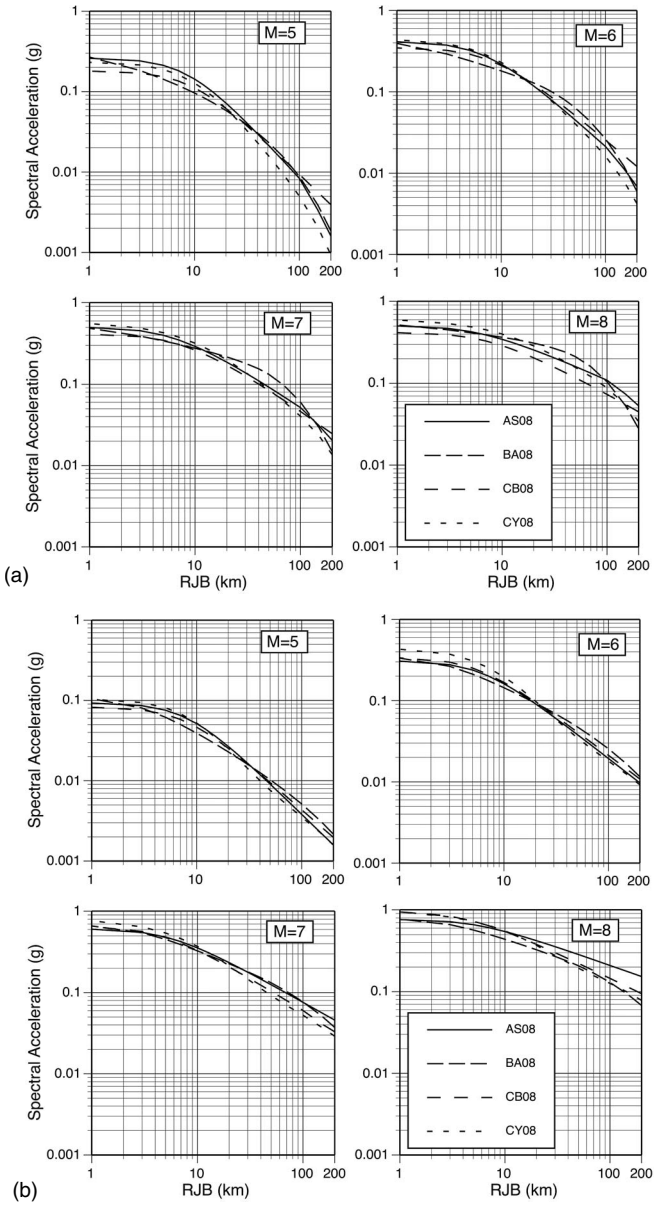

Figure 2. a. Comparison of distance scaling of PGA for strike-slip earthquakes for V_{S30}=270 m/s. b. Comparison of distance scaling of T=1 sec for strike-slip earthquakes for V_{S30}=270 m/s.

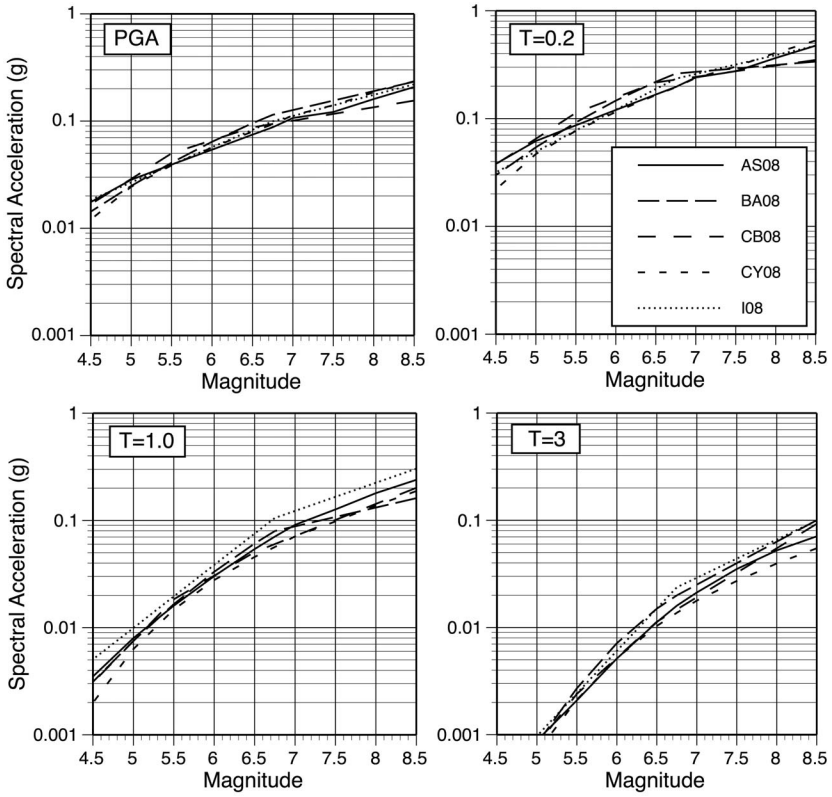

Figure 3. Comparison of magnitude scaling of the median ground motion for strike-slip earthquakes and rock site conditions (V_{S30}=760 m/s) at a distance of 30 km.

MAGNITUDE SCALING

The magnitude scaling of the median ground motion is compared in Figure 3 for an R_{JB} distance of 30 km and a rock site condition. Overall, the magnitude scaling for the five NGA models are very similar. For short spectral periods, the median ground motions are within a factor of 1.5. At long periods, the range increases to a factor of 2 at M5 and M8.

DEPTH OF RUPTURE SCALING

The depth-to-top-of-rupture scaling of the median ground motions is compared in Figure 4 for M6 earthquakes at a R_{JB} distance of 10 km for both strike-slip and reverse earthquakes. For the BA08 model, there is no dependence on depth since the model uses R_{JB} as the distance measure. For the I08 model, there is a systematic decrease in the median ground motion with increasing depth because this model does not include a depth factor and uses R_{rup} as the distance measure. The AS08 and CY08 models include a rupture depth dependence for both strike-slip and reverse earthquakes with the buried

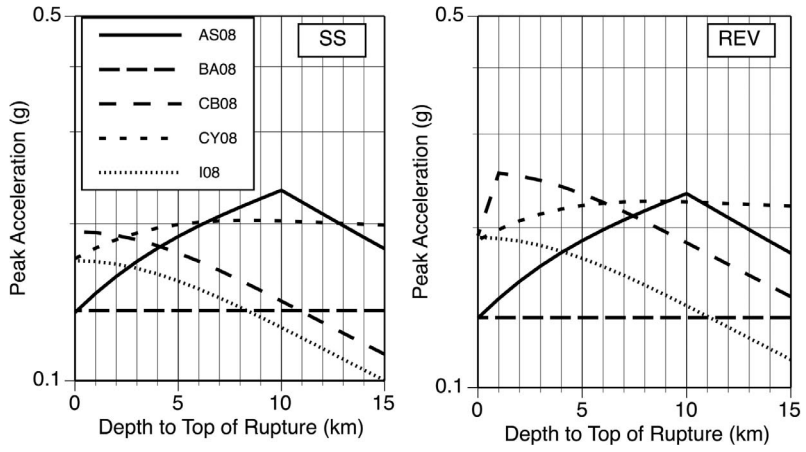

Figure 4. Comparison of scaling of PGA with depth for M6 earthquakes and rock site conditions (V_{S30}=760 m/s) at R_{JB}=10 km: left frame is for strike-slip earthquakes; right frame is for reverse slip earthquakes.

ruptures leading to stronger shaking than surface ruptures at the same distance. As a result of this depth scaling, these two models show an increase in the median ground motion as the rupture depth increases: the CY08 model has a smooth increase from 0 to 7 km depth and then becomes almost constant, similar to the R_{JB} scaling; the AS08 model has a strong scaling with depth with a limit on the depth scaling of 10 km. This causes the AS08 model to have a peak in the scaling at a depth of 10 km. The CB08 model includes a rupture depth effect for reverse earthquakes only for depth greater than 1 km. As a result, the CB08 model shows a systematic decrease in the PGA with increasing depth for strike-slip earthquakes, but there is an increase from surface rupture (depth 0) to 1 km depth (buried rupture) for reverse earthquakes, followed by a smooth decrease.

The range of median ground motions due to the rupture depth scaling is up to a factor of 2. The rupture depth scaling is a new feature of the NGA models. The range can be reduced with the inclusion of additional moderate magnitude (M5-M6) earthquakes to better constrain the rupture-depth scaling.

V_{S30} SCALING

The V_{S30} scaling of the median ground motion is shown in Figures 5a and 5b for M7 strike-slip earthquakes at rupture distances of 100 and 10 km, respectively. For the 100 km distance case, the site response is nearly linear and the four models all show similar $\ln(V_{S30})$ slopes. There are two limits to the V_{S30} scaling. First, there is a limit beyond which the amplification is constant. For the AS08 model this limit is period dependent limit whereas the limit is period independent (1100 m/s) for the CB08 and CY08 models. For the BA08 model, this limit is not included as part of the model. The

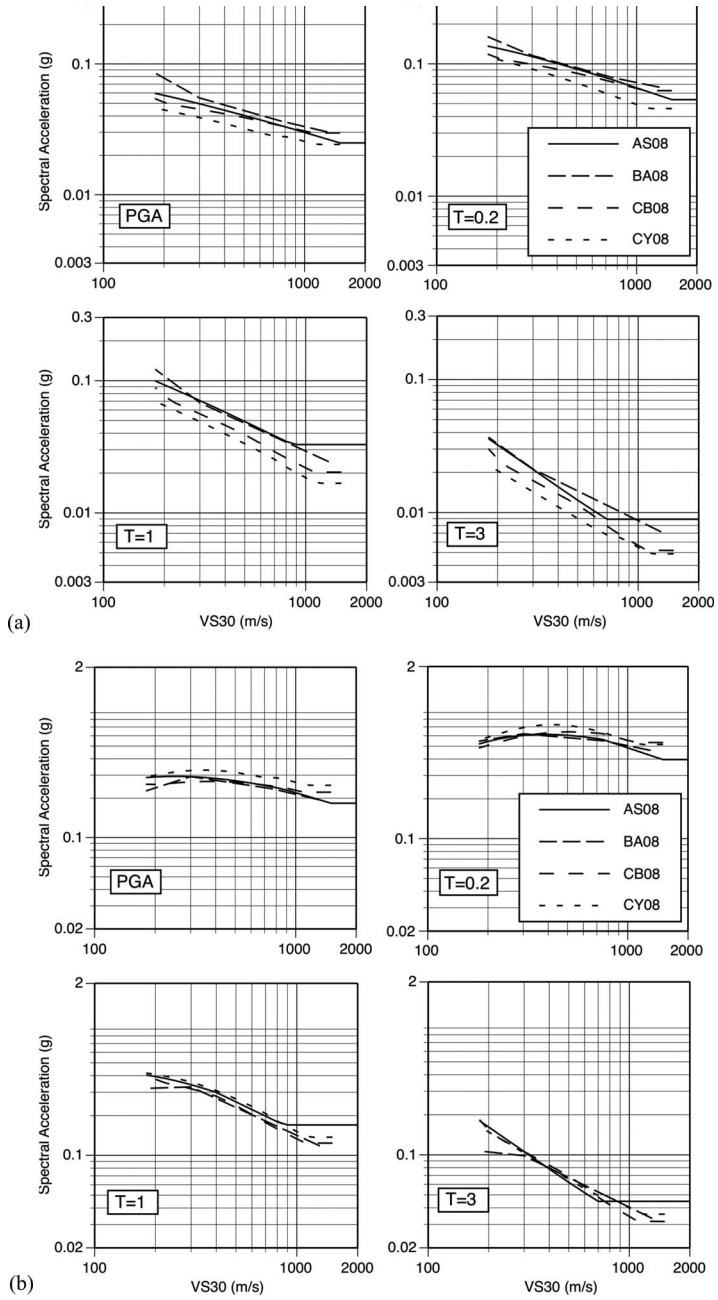

Figure 5. a. Comparison of V_{S30} scaling of the median ground motion for M7 strike-slip earthquakes at a rupture distance of 100 km. b. Comparison of VS30 scaling of the median ground motion for M7 strike-slip earthquakes at a rupture distance of 10 km.

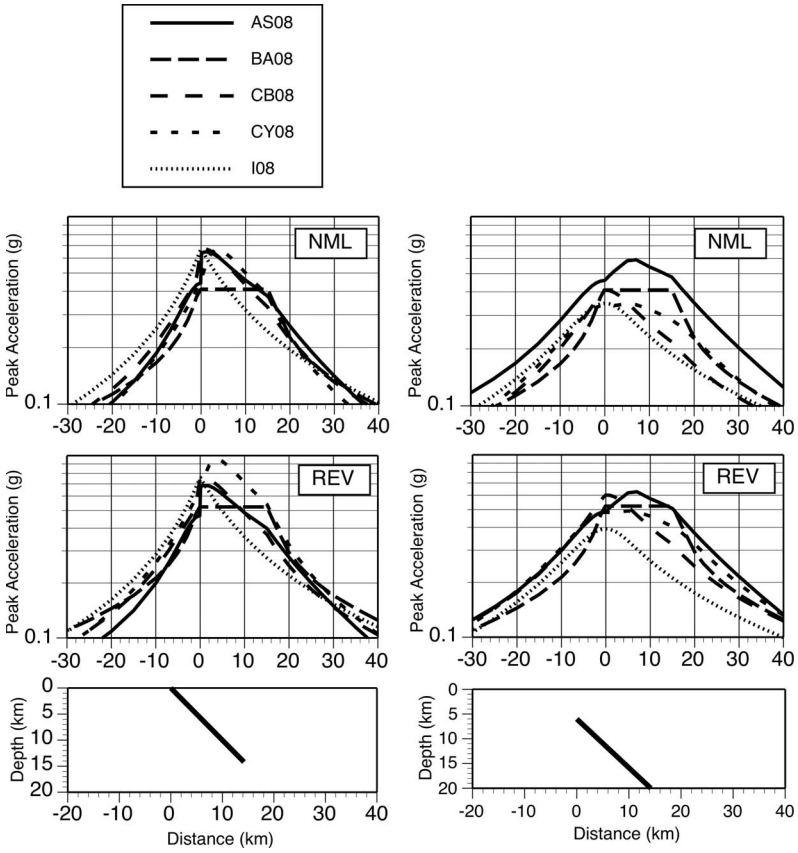

Figure 6. Comparison of FW and HW effects on of PGA for a 45 degree, M6.7 earthquakes for VS30=760 m/s. Left frame: Surface rupture. Right Frame: Buried rupture (top=6 km).

second limit is the maximum V_{S30} for which the models are applicable. The largest V_{S30} values recommended by the developers are 1300 m/s for BA08, 1500 m/s for CB08 and CY08, and 2000 m/s for AS08.

For the 10 km case, there are strong nonlinear effects on the amplification. There is little scaling with V_{S30} for the short periods due to the nonlinear effects. For T=3 sec, the site response is approximately linear and the scaling with V_{S30} is similar to the scaling for the 100 km case.

HANGING-WALL SCALING

The hanging-wall scaling is compared in Figure 6 for reverse and normal M6.7 earthquakes with surface rupture and with buried rupture. For this example, the top of rupture for the buried case is at a depth of 6 km, consistent with the 1994 Northridge earthquake. The AS08, CB08, and CY08 models include explicit HW effects. The BA08

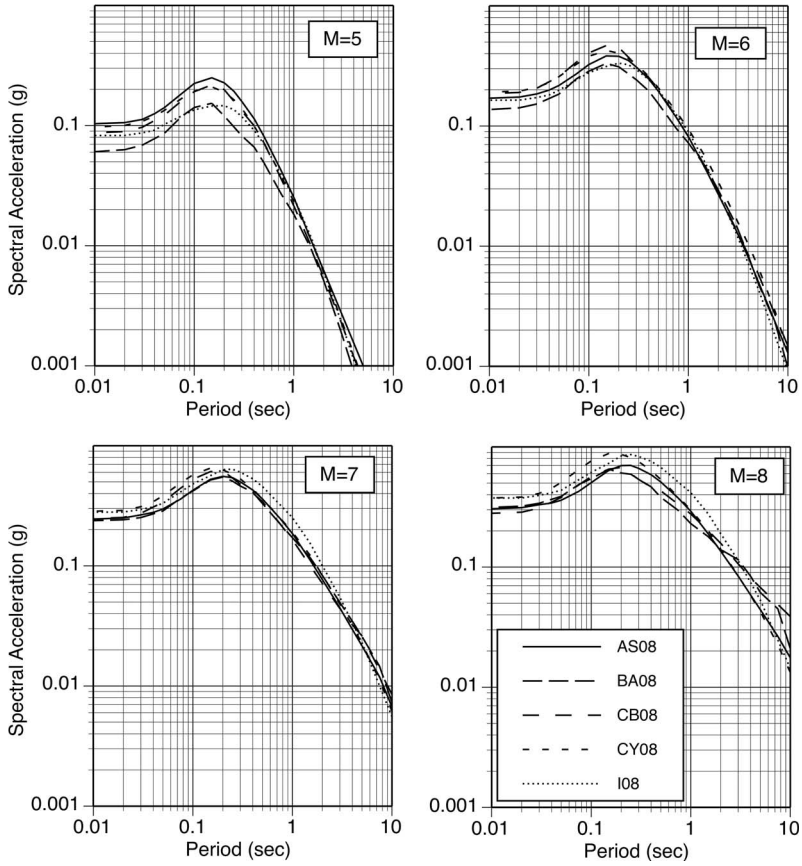

Figure 7. Comparison of median 5% damped spectra for strike-slip earthquakes and rock site conditions (VS30=760 m/s) at an RJB distance of 10 km.

model implicitly includes HW effects through the use of the R_{JB} distance metric which leads to a constant ground motion for sites located over the rupture plane ($R_{JB}=0$). The I08 model does not include HW effects so this model attenuates smoothly as a function of the rupture distance. The buried rupture case leads to the largest differences in the models with a range of a factor of 2.5 in the median ground motions for sites over the HW. The CY08 model has the strongest HW scaling for surface rupture and the AS08 model has the strongest HW scaling for buried ruptures.

RESPONSE SPECTRA

The median response spectra for M=5, 6, 7, and 8 for strike-slip earthquakes for rock site conditions are compared in Figure 7. For M6-M7, the spectral for the five models are similar (within a factor of 1.5). At M5 and M8, the range increases to a factor of 2.

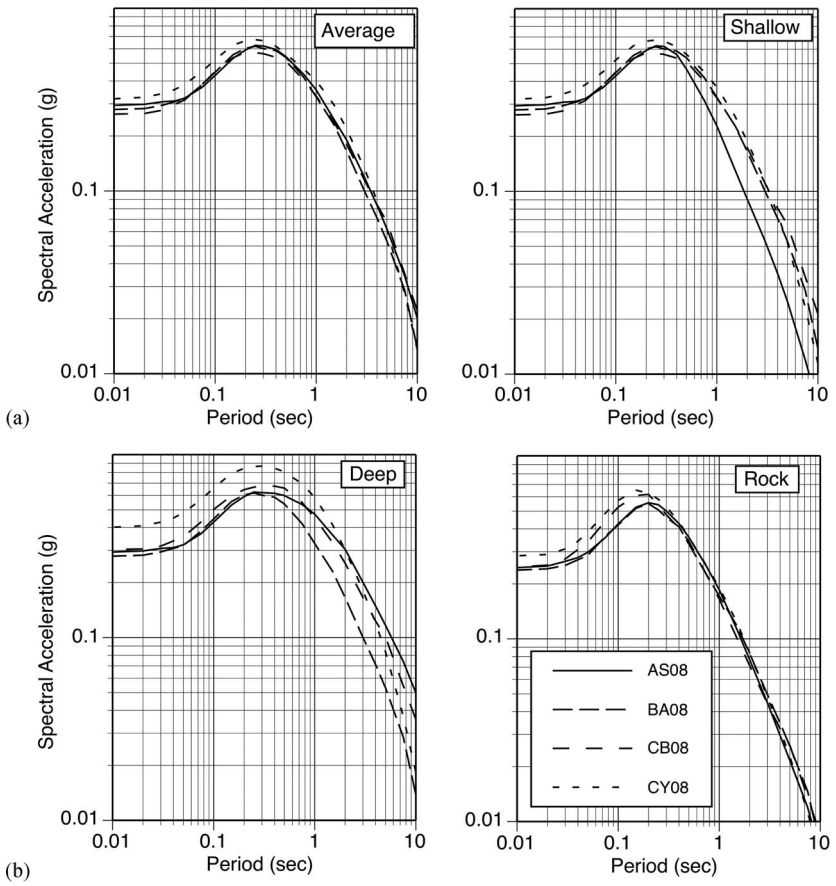

Figure 8. Comparison of median spectra for M7 strike-slip earthquakes at an R_{JB} distance of 10 km for different site conditions: soil sites (V_{S30}=270 m/s) with average soil depth ($Z_{1.0}$=0.5 km, $Z_{2.5}$=2.3 km), shallow soil depth ($Z_{1.0}$=0.1 km, $Z_{2.5}$=0.9 km), and deep soil depth ($Z_{1.0}$=1.2 km, $Z_{2.5}$=4.8 km) depths and rock sites (V_{S30}=760 m/s).

The soil/sediment depth scaling for M7 strike-slip earthquakes at a distance of 10 km is compared in Figure 8. For an average soil/sediment depth ($Z_{1.0}$=0.50 km, $Z_{2.5}$=2.3 km), the four models have very similar spectra (within a factor of 1.3). Three of the models include the effects of soil/sediment depth (the BA08 model does not include soil/sediment depth effects). For shallow soil/sediment depths ($Z_{1.0}$=0.1 km, $Z_{2.5}$=0.9 km), the AS08 model has a large reduction in the long-period ground motion, but the other two models do not have an effect on the long-period ground motion for shallow soil/sediment sites. The AS08 shallow soil/sediment scaling is stronger due to the use of 1-D analytical site response results to constrain the model. For the deep soil/sediment sites ($Z_{1.0}$=1.2 km, $Z_{2.5}$=4.8 km), the three models (AS08, CB08, and CY08) all show a large increase in the long-period motion as compared to the BA08 model that

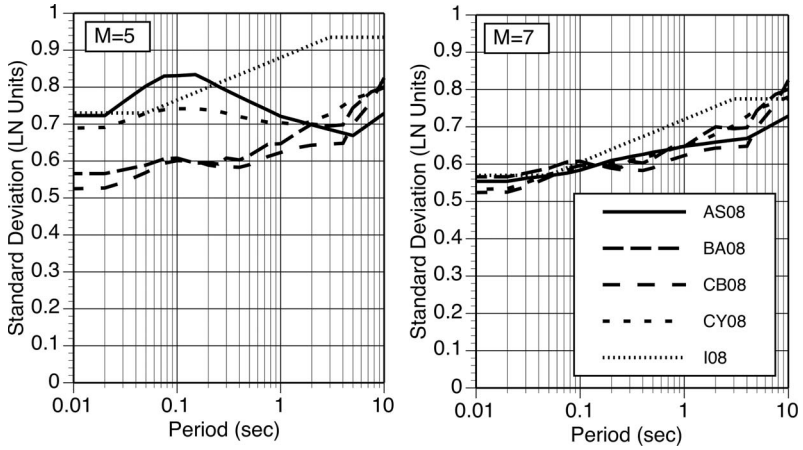

Figure 9. Comparison of the standard deviation for M5 (left) and M7 (right) strike-slip earthquakes at a distance of 30 km for rock site conditions ($V_{S3}0=760$ m/s).

does not include soil/sediment depth scaling. At T=10 sec period, the AS08 and CB08 models show the strongest scaling due to the use of the 3-D analytical basin response results to constrain their models. At short periods, the CB08 and CY08 models show an increase for deep soil/sediment sites based on fitting the scaling seen in the NGA data that have soil/sediment depth estimates.

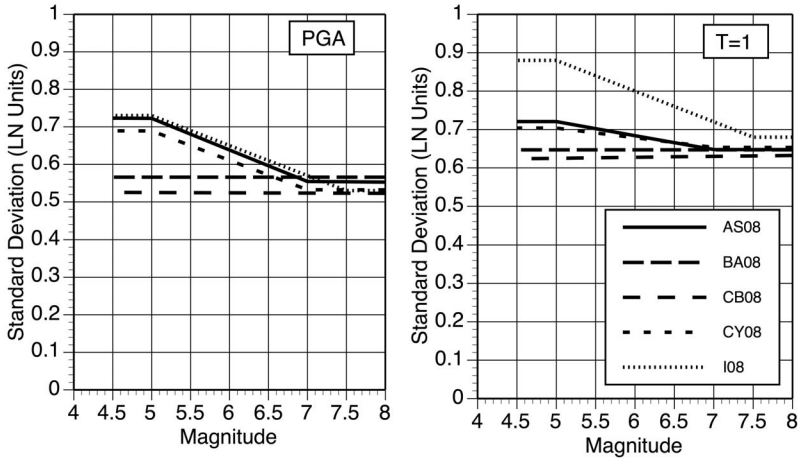

Figure 10. Comparison of magnitude dependence of the standard deviation for PGA (left) and T=1 sec (right) for strike-slip earthquakes at a distance of 30 km for rock site conditions ($V_{S30}=760$ m/s).

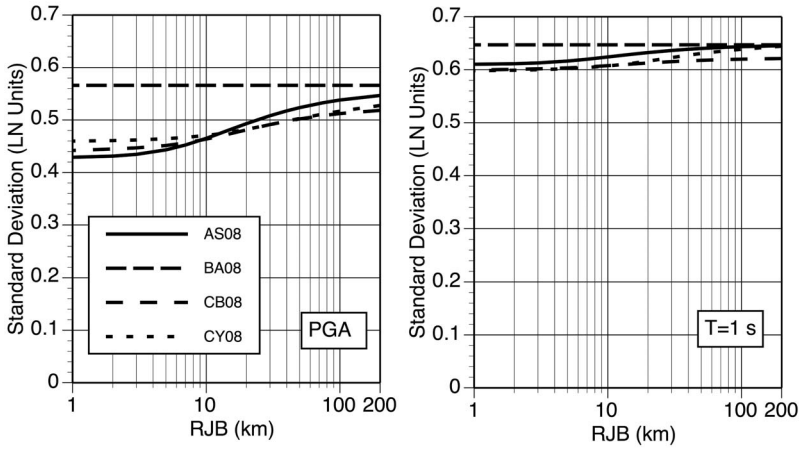

Figure 11. Comparison of distance dependence of the standard deviation for PGA (left) and spectral acceleration at T=1 sec. (right) for M7 strike-slip earthquakes and soil site conditions (V_{S30}=270 m/s).

COMPARISON OF THE STANDARD DEVIATIONS

The period dependence of the standard deviation for M=5 and M=7 earthquakes is compared in Figure 9. For M=7, the five models have similar standard deviations. For M=5, there is a large difference with the three magnitude-dependent models showing much larger standard deviations. The magnitude dependence of the standard deviation is compared in Figure 10 for PGA and T=1 sec. The three models that included a magnitude-dependent standard deviation all included aftershocks, whereas the two models that used a magnitude-independent standard deviation excluded aftershocks. Including aftershocks greatly increases the number of small magnitude earthquakes and the aftershocks show larger variability than the large-magnitude mainshocks.

All four models applicable to soil sites included nonlinear effects on the median site amplification, but they address the impacts on the standard deviation differently. The AS08 and CY08 models include the impacts on both the intra-event and interevent standard deviations. The CB08 model includes the impact on the intra-event standard deviation, but excludes the impact on the interevent standard deviation. The BA08 models does not include the effect on either the intra-event or interevent standard deviations. When the nonlinear effects are included, the standard deviations for the short-period ground motions are reduced. The distance dependence of the standard deviation is shown in Figure 11 for M7 strike-slip earthquakes for PGA and spectral acceleration at T=1 sec. At short distances, the nonlinear effects lead to a reduction of 0.10 to 0.15 natural log units.

CONCLUSIONS

Overall, the NGA models show similar median values (within a factor of 1.5) for vertical strike-slip faults with magnitudes between 5.5 and 7.5. The largest differences are for small magnitudes (M5), very large magnitudes (M8), and sites over the hanging wall. The standard deviations are similar for $M > 6.5$. The largest differences in the standard deviations are for small magnitudes (due to inclusion or exclusion of aftershocks) and for soil sites at short distances (due to inclusion or exclusion of nonlinear effects on the standard deviation).

ACKNOWLEDGMENTS

This study was sponsored by the Pacific Earthquake Engineering Research Center's Program of Applied Earthquake Engineering Research of Lifelines Systems supported by the California Department of Transportation, the California Energy Commission, and the Pacific Gas & Electric Company. This work was partly funded by the PG&E/DOE cooperative agreement: "Development and Verification of an Improved Model for Extreme Ground Motions Produced by Earthquakes" (DOE Award Number DE-FC28-05RW12358).

This work made use of the Earthquake Engineering Research Centers Shared Facilities supported by the National Science Foundation under award number EEC-9701568 through the Pacific Earthquake Engineering Research Center (PEER). Any opinions, findings, and conclusion or recommendations expressed in this material are those of the authors and do not necessarily reflect those of the National Science Foundation.

REFERENCES

Abrahamson, N. A., and Silva, W. J., 2008. Summary of the Abrahamson & Silva NGA ground-motion relations, *Earthquake Spectra* **24**, 67–97.

Boore, D. M., and Atkinson, G. M., 2008. Ground-motion prediction equations for the average horizontal component of PGA, PGV, and 5%-damped PSA at spectral periods between 0.01 s and 10.0 s, *Earthquake Spectra* **24**, 99–138.

Campbell, K. W., and Bozorgnia, Y., 2006. Next generation attenuation (NGA) empirical ground motion models: can they be used in Europe?, *First European Conference on Earthquake Engineering and Seismology Geneva, Switzerland*, 3–8 September 2006, Paper: 458.

——, 2008. NGA ground motion model for the geometric mean horizontal component of PGA, PGV, PGD and 5% damped linear elastic response spectra for periods ranging from 0.01 to 10 s, *Earthquake Spectra* **24**, 139–171.

Chiou, B. S. J., and Youngs, R. R., 2008. Chiou-Youngs NGA ground motion relations for the geometric mean horizontal component of peak and spectral ground motion parameters, *Earthquake Spectra* **24**, 173–215.

Choi, Y., and Stewart, J. P., 2005. Nonlinear site amplification as function of 30 m shear-wave velocity, *Earthquake Spectra* **21**, 1–30.

Day, S. M., Bielak, J., Dreger, D., Graves, R., Larsen, S., Olsen, K., and Pitarka, A., 2005. *3D*

ground motion simulations in basins, *Final report prepared for the Pacific Earthquake Engineering Research Center*, Project 1A03.

Idriss, I. M., 2008. An NGA empirical model for estimating the horizontal spectral values generated by shallow crustal earthquakes, *Earthquake Spectra* **24**, 217–242.

Silva, W. J., 2005. Site response simulations for the NGA project, *Report prepared for the Pacific Earthquake Engineering Research Center*.

Stafford, P. J., Strasser, F. O., and Bommer, J. J., 2008. An evaluation of the applicability of the NGA models to ground-motion prediction in the Euro-Mediterranean region, *Bulletin of Earthquake Engineering* **6**, 144–177.

Walling, M., Silva, W. J., and Abrahamson, N. A., 2008. Nonlinear site amplification factors for constraining the NGA models, *Earthquake Spectra* **24**, 243–255.

(Received 20 December 2007; accepted 13 February 2008)